

WHY BARYONS MATTER: THE KINEMATICS OF DWARF SPHEROIDAL SATELLITES

ALYSON M. BROOKS¹, ADI ZOLOTOV²

(Dated: July 12, 2012)

Submitted for publication in ApJ Letters

ABSTRACT

We use some of the highest resolution cosmological simulations ever produced of Milky Way-mass galaxies that include both baryons and dark matter to show that baryonic physics (energetic feedback from supernovae and subsequent tidal stripping) significantly reduces the dark matter mass in the central regions of luminous satellite galaxies. The reduced central masses of the simulated satellites reproduce the observed internal dynamics of Milky Way and M31 satellites as a function of luminosity. Including baryonic physics in Cold Dark Matter models naturally explains the observed low dark matter densities in the Milky Way's dwarf spheroidal population. Our simulations therefore resolve the tension between kinematics predicted in Cold Dark Matter theory and observations of satellites, without invoking alternative forms of dark matter.

1. INTRODUCTION

There are fewer small satellite galaxies orbiting our Milky Way galaxy than predicted by the favored Cold Dark Matter (CDM) cosmological model (Moore et al. 1999; Klypin et al. 1999). Theories often reconcile the discrepancy between the number of observed satellites and CDM predictions by invoking the suppression of star formation in low mass galaxies, for example by UV heating at reionization (e.g., Okamoto et al. 2008). If only the most massive satellites form stars, this can bring the predicted number of luminous satellites down from thousands to tens, in line with observations. Even then a serious problem remains, as the most massive satellites predicted by CDM models are still much too dense compared to what we observe (Boylan-Kolchin et al. 2011, 2012; Wolf & Bullock 2012; Hayashi & Chiba 2012). The tension between the observations and the predictions of the CDM model have led some researchers to propose exotic or alternative forms of dark matter to reduce the central masses of satellites (Vogelsberger et al. 2012; Lovell et al. 2012). However, the highest resolution simulations available to date to study the internal properties of satellites include only the dark matter (DM) component of galaxies, neglecting the effects of baryons (e.g., Diemand et al. 2007; Springel et al. 2008; Boylan-Kolchin et al. 2012).

Studies using high resolution simulations that include baryons have shown that star formation and subsequent supernova feedback can alter the DM structure at the center of galaxies (Navarro et al. 1996; Read & Gilmore 2005; Mashchenko et al. 2006; Governato et al. 2010; Cloet-Osselaer et al. 2012; Macciò et al. 2012; Pontzen & Governato 2012; Governato et al. 2012; Zolotov et al. 2012; Teyssier et al. 2012). Governato et al. (2010) and Pontzen & Governato (2012) demonstrated that high resolution alone is not sufficient to capture the effects of baryons on DM. Rather, it is necessary to adopt a

realistic treatment of star formation that restricts stars to form only in high density regions comparable to giant molecular clouds. The subsequent supernova (SN) feedback then naturally creates over-pressurized regions of hot gas that rapidly expand, flattening the potential at the center of galaxies, leading to an irreversible expansion in the DM orbits. Multiple bursts of star formation push more DM to larger radii, transforming an initially steep, cuspy DM density profile into a cored profile (Governato et al. 2012).

Zolotov et al. (2012) are the first to examine how this impact of baryons on the DM structure affects the evolution of satellites around a Milky Way-massed galaxy. They demonstrate that SN feedback reduces the central DM densities of satellites with $M_* \gtrsim 10^7 M_\odot$ before infall. After infall, the presence of a baryonic disk increases the mass loss rate via tidal stripping for all satellites (Zolotov et al. 2012; Peñarrubia et al. 2010). This tidal effect is particularly strong for those satellites that enter with cored DM halos, further increasing the discrepancy in the central masses predicted by DM+baryon and DM-only simulations. In this Letter we examine the effect that this evolution has on the observed properties of the satellite population in Milky Way-mass galaxies at $z = 0$. We then use our results to interpret the observed dynamics of the Milky Way and M31 dwarf Spheroidal (dSph) satellites.

2. THE SIMULATIONS

The satellite sample that we use here is drawn from Zolotov et al. (2012), and we refer the reader to that paper for full details of the simulations and satellite selection. Briefly, two halos with virial masses of $7 \times 10^{11} M_\odot$ and $8 \times 10^{11} M_\odot$ at $z = 0$ were run with and without baryons. The DM-only simulations were run with PKDGRAV (Stadel 2001), while the simulations with baryons were run with PKDGRAV's N-Body + Smoothed Particle Hydrodynamics (SPH) successor, GASOLINE (Wadsley et al. 2004).

In the SPH runs, gas can cool via primordial and metal lines following Shen et al. (2010). A prescription for creation and destruction of H_2 is implemented following Christensen et al. (2012), and star formation is

¹Department of Astronomy, University of Wisconsin-Madison, 475 N. Charter St., Madison, WI 53706; abrooks@astro.wisc.edu

²Racah Institute of Physics, The Hebrew University, Jerusalem, Israel 91904; adizolotov@gmail.com

TABLE 1
 $z = 0$ SATELLITE PROPERTIES

Satellite ID	M_{stellar} $10^7 M_{\odot}$ (1)	M_V (2)	M_{HI} M_{\odot} (3)	v_{max} km/s (4)
h258, sat1	4.7	-13.7	3.5e5	35
h258, sat2	2.0	-12.8	3.4e5	27
h258, sat3	1.9	-12.6	737.5 ^a	24
h258, sat4	3.4	-13.3	0.	20
h258, sat5	2.9	-13.0	0.	15
h258, sat6	0.5	-11.3	1.2e5	19
h258, sat7	1.1	-12.1	0.	20
h258, sat8	.06	-9.0	0.	20
h258, sat9	.14	-9.9	0.	16
h258, sat10	.05	-8.8	0.	17
h258, sat11	.32	-10.7	0.	12
h258, sat12	.10	-9.5	0.	14
h258, sat13	.16	-10.1	0.	13
h277, sat1	7.4	-14.7	3.2e7	36
h277, sat2	4.0	-13.9	3.8e7	33
h277, sat3	8.8	-14.3	5.1e6	19
h277, sat4	3.7	-13.4	1.3e6	28
h277, sat5	.25	-10.4	0.	15
h277, sat6	.31	-10.6	0.	7
h277, sat7	.14	-9.9	0.	11

NOTE. — Column (1) total stellar mass in the satellite. Column (2) corresponding V -band magnitude, based on the age and metallicity of star particles using the Starburst99 stellar population synthesis models (Vázquez & Leitherer 2005). Column (3) mass in HI gas in the satellite. Column (4) maximum circular velocity, v_{max} .

^a This mass of HI would remain undetected by current HI surveys.

tied directly to the presence of H_2 gas. A uniform UV background turns on at $z = 9$, mimicking reionization (Haardt & Madau 2001). Supernovae deposit 10^{51} ergs of thermal energy into the surrounding gas following the “blastwave” scheme described in Stinson et al. (2006).

Zolotov et al. (2012) show that the $z = 0$ satellite populations of both galaxies are in good agreement with the Milky Way (MW) and M31 satellite luminosity functions, from $-8 < M_V < -15$. Properties of the satellites in this luminosity range are listed in Table 1, including a few that are still gas-rich at $z = 0$. This range excludes from each simulation one brighter, Magellanic-like satellite. All but one of the gas-free SPH satellites studied here have been matched to a satellite counterpart in the DM-only run. In the remainder of the paper, we report kinematic values at 1 kpc for the simulations in order to both ensure convergence of the rotation curve, and as a useful comparison to the observations that have kinematic data measured at $\lesssim 1$ kpc.

2.1. Baryonic Evolution with Mass

With the exception of three of the lowest mass halos, all of the satellite progenitors retain gas until infall, allowing their star formation histories (SFHs) to extend at least until infall (in line with observational data, see Grebel & Gallagher 2004; Dellenbusch et al. 2008; Weisz et al. 2011). However, the nature of the star formation varies with halo mass. Heating from the uniform UV background, combined with early star formation and SN feedback, removes a substantial amount of gas from halos below $10^9 M_{\odot}$, leaving them gas poor. These halos lose 10 – 90 times more mass in gas than stars formed by the time of their accretion. The remaining gas has

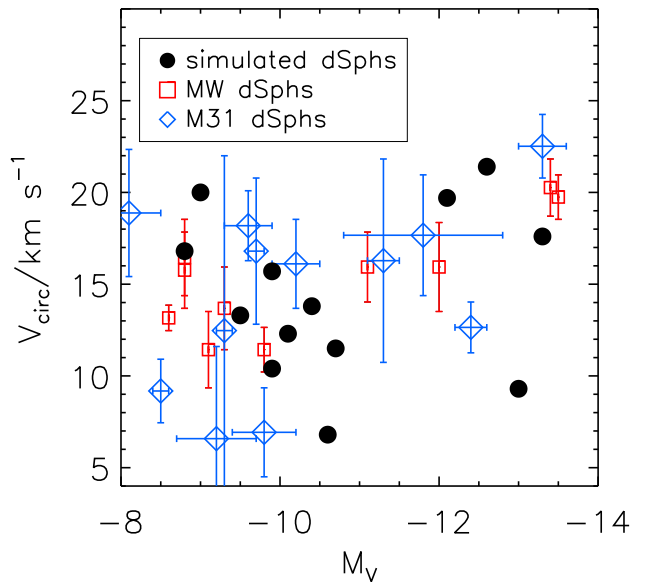


FIG. 1.— The total v_c at 1 kpc for the SPH satellites as a function of their V -band magnitude, at $z = 0$. The empty red squares and empty blue diamonds are v_c at the half light radii for MW and M31 dSphs, respectively.

low surface densities and is inefficient at producing stars. The low level of star formation that can occur prior to infall is relatively constant rather than stochastic.

Halos above $10^9 M_{\odot}$, corresponding to halos with $M_* > 10^7 M_{\odot}$ at infall, are able to retain more of their gas for longer, allowing them to have extended SFHs. Unlike the lower mass satellites, the SFHs of massive satellites tend to be episodic and bursty. With their deeper potential wells, the more massive halos achieve an initially higher star formation rate (SFR) than the lower mass halos as gas cools in the central galaxy. The subsequent SN feedback from the burst heats the surrounding gas, shutting off star formation for a period of time until the gas can again cool and continue with another burst. These bursty SFHs lead to DM core creation prior to infall (Zolotov et al. 2012).

Many subhalos lose most of their gas after infall and are gas-free by $z = 0$ (see Table 1).³ While some subhalos lose their gas nearly instantly at infall, some are capable of retaining their gas for an extended time, and even having a low level of star formation. However, the SFRs become strongly suppressed after infall, and no subhalo continues to undergo the bursty star formation that contributes to DM core creation. Instead, the mass within 1 kpc is substantially reduced when gas is stripped after infall.

3. INTERPRETING OBSERVED DWARF SPHEROIDALS

Below we discuss the observational properties of the Milky Way and M31 dSphs in light of results that show that baryonic effects can reduce the central DM masses of luminous satellites that infall to a $\sim L^*$ galaxy.

³ Satellites that retain gas until $z = 0$ may be artificially gas-rich, due to inefficient stripping of gas in SPH (Agertz et al. 2007).

3.1. Satellite Kinematics at Redshift 0

Figure 1 shows the total v_c at 1 kpc of the gas-free SPH satellites (dSph analogs, black circles) as a function of M_V . Plotted with the simulation data are observational results for dSphs with M_V brighter than -8 in both the MW from Walker et al. (2009) and M31 from Tollerud et al. (2012), and supplemented by the compilation of McConnachie (2012) for And II and And VI. For the observational data, $v_c(r_{1/2}) = \sqrt{3\sigma^2}$, where σ is the line of sight stellar velocity dispersion, and $r_{1/2}$ is the half-light radius of the dSph. Walker et al. (2009) and Wolf et al. (2010) have shown that assumptions about isotropy are minimized at $r_{1/2}$, making the masses determined at $r_{1/2}$ the most robust. The half-light radii are $\lesssim 1$ kpc for all of the observed dSph. Our measurements for the simulated gas-free satellites are upper limits to the values derived at typical half light radii, as the rotation curves of these satellites either peak or continue to rise at 1 kpc.

Figure 1 shows that all of the v_c values for the simulated gas-free satellites are less than 22 km/s, consistent with v_c results for MW and M31 dSphs. In contrast, of the 12 matched DM-only counterparts to the SPH satellites, nine have $20 < v_c(1\text{kpc}) < 34$ km/s, grossly inconsistent with the MW and M31 dSph data. Previous studies using DM-only simulations have found that subhalos simulated in a CDM-context are significantly more dense than observations of the MW dSphs suggest (Boylan-Kolchin et al. 2011, 2012; Wolf & Bullock 2012; Hayashi & Chiba 2012). Zolotov et al. (2012), however, have shown that the central 1 kpc of dwarf satellites can be strongly affected by both SN feedback and tidal stripping, reducing their central DM densities. When these baryonic effects are modeled self-consistently, as they are here, the kinematics of simulated satellites are well-matched to the observed kinematics of dSph satellites.

Figure 2 shows the difference in the DM contribution to v_c at 1 kpc between the SPH runs used here and the identical DM-only runs that neglect baryonic effects, as a function of M_V of the SPH satellites at $z = 0$. It is important to note that these results include both the effects of SN feedback on the DM distribution of the satellites *prior* to infall, and tidal stripping *after* infall. In order to quantify the change in DM mass that this combination produce in the central regions of satellites compared to the DM-only case, we fit a linear regression to the data points in Figure 2. The resulting fit is shown by the dotted line, and yields $\Delta(v_{c,1\text{kpc}}) = -10.47 - 1.35 \times M_V$. The y-axis range of Figure 2 excludes from the plot one outlier with $\Delta(v_c) \sim 25$ km/s.⁴

Figure 2 demonstrates the amount by which DM-only simulations over-predict the central DM masses of satellite galaxies, and hence why such simulations find that their satellites are inconsistent with the kinematics of the MW dSphs. An explicit example of the change quantified in Figure 2 is demonstrated in Figure 3. The total rotation curve (DM and baryonic mass) for an SPH simulated subhalo is shown in Figure 3, which closely matches

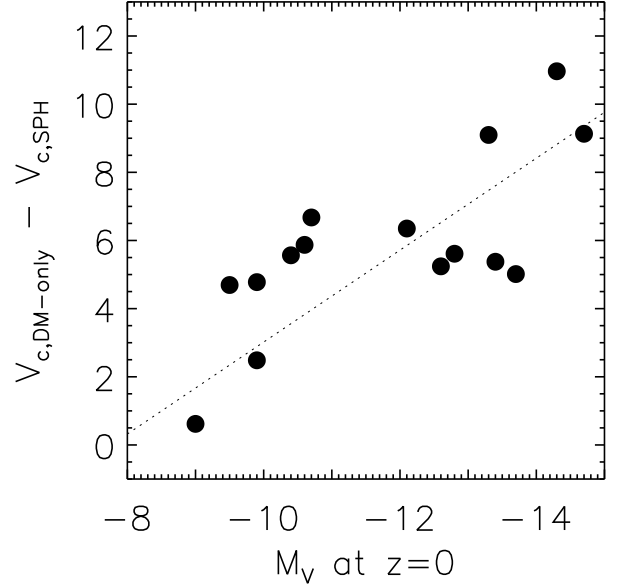


FIG. 2.— The difference in v_c of the DM rotation curves at 1 kpc between the SPH and DM-only simulations, as a function of the V-band magnitude in the SPH satellites, for all satellites listed in Table 1. The dotted line is a linear fit to the points.

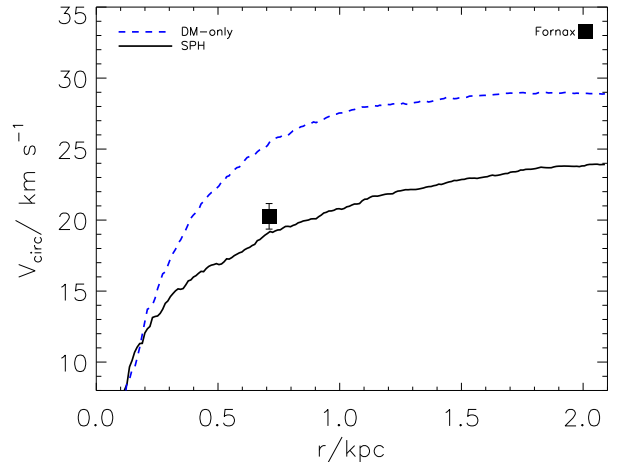


FIG. 3.— The $z = 0$ rotation curves of a simulated satellite and its DM-only counterpart. The v_c for Fornax is over-plotted, based on the data in Walker et al. (2009). The combination of SN feedback (before infall) and tidal stripping (after infall) substantially lower the v_c of the SPH satellite by $z = 0$, and is in good agreement with the observed v_c of Fornax.

the derived v_c at the half light radius of Fornax, along with the rotation curve for the same subhalo in a DM-only run without baryons. The DM-only satellite clearly over-predicts the central mass of this satellite. For almost all of our satellites, the *DM-only runs produce satellites with 2-4 times more mass in the central 1 kpc than their SPH counterparts.*

It is common when making predictions for the properties of subhalos within the CDM model to associate the most massive DM-only subhalos at infall with the most luminous satellites at $z = 0$ (e.g., Koposov et al.

⁴ This outlier recently passed directly through the disk of its parent galaxy, which doesn't exist in the DM-only run, making $\Delta(v_c)$ for this galaxy larger than in other satellites.

2009; Boylan-Kolchin et al. 2011, 2012), i.e., an abundance matching technique. Indeed, the most massive subhalos in the DM-only runs in this work are matched to the most luminous satellites in the SPH runs at infall (Zolotov et al. 2012). However, SPH satellites experience evolution that DM-only runs do not account for. It is therefore incorrect to assume that the central masses of DM-only subhalos should predict the observed masses in the inner regions of luminous subhalos. For example, the DM-only satellite shown in Figure 3 is a massive subhalo that would be assumed to host a luminous dSph at $z = 0$. However, this assignment would over-predict the central mass of this satellite by factors of a few.

3.2. The Scatter in v_c

A long-standing puzzle in the observational data is that some of the bright MW dSphs with $M_V \sim -13$ have similar v_c values to some of the much fainter galaxies with $M_V \sim -8$. In the field, galaxies display a clear trend of increasing stellar mass with halo mass (e.g., Moster et al. 2012), yet satellites that span two orders of magnitude in luminosity seem to show no trend in their central v_c with mass. The comparable velocities of Draco ($M_V = -8.8$), and Fornax ($M_V = -13.4$), for example, have led Peñarrubia et al. (2008) to conclude that Draco formed in a halo 5 times more massive than Fornax, despite being 70 times fainter.

The simulated SPH satellites shown in Figure 1 follow a similar trend to the observed MW and M31 dSphs; at $z = 0$ simulated satellites with $M_V = -9$ can have comparable kinematics to satellites with $M_V = -13$. At infall, however, SPH satellites follow an increasing trend of stellar mass with halo mass, with $M_* \propto M_{vir}^2$. The strong trend seen at infall (and in the field) is erased in the subsequent tidal evolution of these satellites, resulting in the scatter observed at $z = 0$.

Since both SPH and DM-only satellites undergo tidal stripping, one might expect that SPH and DM-only satellites would display a similar scatter in v_c at $z = 0$. However, when DM-only satellites are matched to the stellar mass of their SPH counterparts, DM-only satellites still show a trend of increasing v_c at 1 kpc with luminosity at $z = 0$, unlike satellites simulated with baryons. There are two effects that lead to this divergence between SPH and DM-only satellites. First, the presence of a baryonic disk in the SPH runs (the DM-only runs don't have a disk) enhances the rate of mass lost at each pericentric passage for all SPH satellites. This effect is increasingly significant with increasing time after infall and for satellites on more eccentric orbits (Peñarrubia et al. 2010; Zolotov et al. 2012). For example, our sample contains three low luminosity satellites ($M_V > -11$) that are on highly eccentric orbits. These SPH satellites undergo a greater reduction in their mass and central v_c than satellites on circular orbits. This results in the large spread of v_c values for simulated SPH satellites fainter than $M_V \sim -11$, similar to the observational data in Figure 1. Second, the influence of a baryonic disk is especially strong for satellites with shallow DM density profiles, like the SPH satellites in our sample brighter than $M_V \sim -12$. This effect exacerbates the amount of central mass lost in the most luminous subhalos, and contributes to lowering the central v_c of these satellites to under 25 km/s. These combined effects lead to satellites

across the luminosity range that appear to have similar masses at $z = 0$. Without the effect of the disk, and with their steep density profiles, DM-only satellites experience overall less mass loss for a given orbit, and therefore tidal effects do not introduce a large scatter in their v_c .

4. CONCLUSIONS & DISCUSSION

We have demonstrated that simulations that account for the effects of SN feedback and enhanced tidal stripping on satellites result in a satellite population whose kinematic properties match the observed properties of the Milky Way and M31 satellites. Our findings are in sharp contrast to studies using DM-only simulations, which over-predict the central masses of satellites in comparison to observations.

Our results predict:

1. All dSph satellites brighter than $M_V \sim -12$ should have central DM density slopes that are shallow (or cored) out to ~ 1 kpc, and total masses several factors lower than predicted by CDM DM-only simulations.
2. If a satellite fainter than $M_V \sim -12$ underwent substantial stripping ($\sim 90\%$ of its total mass, Peñarrubia et al. 2008), it could have started off as a more luminous dSph with a DM core.
3. The presence of cored density profiles at radii under ~ 500 pc in satellites fainter than $M_V \sim -12$ is not ruled out by our simulations, as we do not resolve this region.
4. Regardless of the density profile, the tidal effects of the disk can dramatically lower the central DM mass of any satellite, depending on infall time and orbital eccentricity.

Most attempts to measure the central density slopes of dSphs have relied on using the spherical Jeans equations (e.g., Gilmore et al. 2007), but the mass and anisotropy of the stellar orbits are degenerate in the Jeans model, making the results highly dependent on adopted assumptions (Evans et al. 2009). Recent works (Wolf & Bullock 2012; Hayashi & Chiba 2012) have attempted to overcome this issue by searching for maximum likelihoods in parameter space, but still adopt Jeans modeling. Schwarzschild modeling avoids some of the assumptions inherent in Jeans modeling, and has been applied to Fornax and Sculptor, with the conclusion that both have cored DM density profiles (Jardel & Gebhardt 2012; Breddels et al. 2012).

Alternatively, studying dSphs that have multiple stellar populations that span varying radii avoids any assumption about a mass model or isotropy, allowing a direct fit to two independent derivations of the mass. The central density slopes of Fornax and Sculptor have been determined with this method (Walker & Peñarrubia 2011; Amorisco & Evans 2012; Battaglia et al. 2008; Agnello & Evans 2012), with all studies concluding that both Fornax (with slope measured out to ~ 1 kpc) and Sculptor (measured interior to 500 pc) favor cored density profiles, and exclude cuspy density profiles at high significance. It has also been argued that the

fact that Fornax’s globular cluster orbits have not decayed by dynamical friction requires a cored DM profile (Goerdt et al. 2006; Cole et al. 2012).

Higher resolution simulations will be necessary to predict if small (on scales < 500 pc) DM cores exist in lower luminosity satellites, though the observational evidence (e.g., in Sculptor, Walker & Peñarrubia 2011) suggests that they exist. We note that the substantial reduction in the overall normalization of the central DM densities of satellites due to the presence of a disk will lead to a reduced DM annihilation signal. This suggests that deeper searches for DM annihilation could help to constrain the central masses of these objects. However, it is already clear that the overall concentrations of the MW dSph population are lower than predicted by CDM DM-only simulations (Boylan-Kolchin et al. 2012; Wolf & Bullock 2012; Hayashi & Chiba 2012). The lowered densities of our simulated satellites are consistent with these observational results.

We thank Michael Boylan-Kolchin, Alan McConnachie, Louie Strigari, and Matt Walker for useful discussions. AB acknowledges support from The Grainger Foundation. AZ acknowledges support from the Lady Davis Foundation. This material is based upon work supported in part by the National Science Foundation Grant No. 1066293 and the hospitality of the Aspen Center for Physics. AZ’s work was partially supported by the ISF grant 6/08, by GIF grant G-1052-104.7/2009, by the DFG grant STE1869/1-1.GE625/15-1. Resources supporting this work were provided by the NASA High-End Computing (HEC) Program through the NASA Advanced Supercomputing (NAS) Division at Ames Research Center. We thank Charlotte Christensen, Fabio Governato, Tom Quinn, Sijing Shen, and James Wadsley for use of the GASOLINE code and simulations.

REFERENCES

- Agertz, O. et al. 2007, *MNRAS*, 380, 963
 Agnello, A., & Evans, N. W. 2012, *ArXiv e-prints*
 Amorisco, N. C., & Evans, N. W. 2012, *MNRAS*, 419, 184
 Battaglia, G., Helmi, A., Tolstoy, E., Irwin, M., Hill, V., & Jablonka, P. 2008, *ApJ*, 681, L13
 Boylan-Kolchin, M., Bullock, J. S., & Kaplinghat, M. 2011, *MNRAS*, 415, L40
 —. 2012, *MNRAS*, 2657
 Breddels, M. A., Helmi, A., van den Bosch, R. C. E., van de Ven, G., & Battaglia, G. 2012, in *European Physical Journal Web of Conferences*, Vol. 19, European Physical Journal Web of Conferences, 3009
 Christensen, C., Quinn, T., Governato, F., Stilp, A., Shen, S., & Wadsley, J. 2012, *ArXiv e-prints*
 Cloet-Osselaer, A., De Rijcke, S., Schroyen, J., & Dury, V. 2012, *MNRAS*, 2952
 Cole, D. R., Dehnen, W., Read, J. I., & Wilkinson, M. I. 2012, *ArXiv e-prints*
 Dellenbusch, K. E., Gallagher, III, J. S., Knezek, P. M., & Noble, A. G. 2008, *AJ*, 135, 326
 Diemand, J., Kuhlen, M., & Madau, P. 2007, *ApJ*, 667, 859
 Evans, N. W., An, J., & Walker, M. G. 2009, *MNRAS*, 393, L50
 Gilmore, G., Wilkinson, M., Kleyna, J., Koch, A., Evans, W., Wyse, R. F. G., & Grebel, E. K. 2007, *Nuclear Physics B Proceedings Supplements*, 173, 15
 Goerdt, T., Moore, B., Read, J. I., Stadel, J., & Zemp, M. 2006, *MNRAS*, 368, 1073
 Governato, F. et al. 2010, *Nature*, 463, 203
 —. 2012, *ArXiv e-prints*
 Grebel, E. K., & Gallagher, III, J. S. 2004, *ApJ*, 610, L89
 Haardt, F., & Madau, P. 2001, in *Clusters of Galaxies and the High Redshift Universe Observed in X-rays*, ed. D. M. Neumann & J. T. V. Tran
 Hayashi, K., & Chiba, M. 2012, *ArXiv e-prints*
 Jardel, J. R., & Gebhardt, K. 2012, *ApJ*, 746, 89
 Klypin, A., Kravtsov, A. V., Valenzuela, O., & Prada, F. 1999, *ApJ*, 522, 82
 Koposov, S. E., Yoo, J., Rix, H.-W., Weinberg, D. H., Macciò, A. V., & Escudé, J. M. 2009, *ApJ*, 696, 2179
 Lovell, M. R. et al. 2012, *MNRAS*, 420, 2318
 Macciò, A. V., Stinson, G., Brook, C. B., Wadsley, J., Couchman, H. M. P., Shen, S., Gibson, B. K., & Quinn, T. 2012, *ApJ*, 744, L9
 Mashchenko, S., Couchman, H. M. P., & Wadsley, J. 2006, *Nature*, 442, 539
 McConnachie, A. W. 2012, *AJ*, 144, 4
 Moore, B., Ghigna, S., Governato, F., Lake, G., Quinn, T., Stadel, J., & Tozzi, P. 1999, *ApJ*, 524, L19
 Moster, B. P., Naab, T., & White, S. D. M. 2012, *ArXiv e-prints*
 Navarro, J. F., Eke, V. R., & Frenk, C. S. 1996, *MNRAS*, 283, L72
 Okamoto, T., Gao, L., & Theuns, T. 2008, *MNRAS*, 390, 920
 Peñarrubia, J., Benson, A. J., Walker, M. G., Gilmore, G., McConnachie, A. W., & Mayer, L. 2010, *MNRAS*, 406, 1290
 Peñarrubia, J., McConnachie, A. W., & Navarro, J. F. 2008, *ApJ*, 672, 904
 Pontzen, A., & Governato, F. 2012, *MNRAS*, 421, 3464
 Read, J. I., & Gilmore, G. 2005, *MNRAS*, 356, 107
 Shen, S., Wadsley, J., & Stinson, G. 2010, *MNRAS*, 1043
 Springel, V. et al. 2008, *MNRAS*, 391, 1685
 Stadel, J. G. 2001, PhD thesis, UNIVERSITY OF WASHINGTON
 Stinson, G., Seth, A., Katz, N., Wadsley, J., Governato, F., & Quinn, T. 2006, *MNRAS*, 373, 1074
 Teyssier, R., Pontzen, A., Dubois, Y., & Read, J. 2012, *ArXiv e-prints*
 Tollerud, E. J. et al. 2012, *ApJ*, 752, 45
 Vázquez, G. A., & Leitherer, C. 2005, *ApJ*, 621, 695
 Vogelsberger, M., Zavala, J., & Loeb, A. 2012, *ArXiv e-prints*
 Wadsley, J. W., Stadel, J., & Quinn, T. 2004, *New Astronomy*, 9, 137
 Walker, M. G., Mateo, M., Olszewski, E. W., Peñarrubia, J., Wyn Evans, N., & Gilmore, G. 2009, *ApJ*, 704, 1274
 Walker, M. G., & Peñarrubia, J. 2011, *ApJ*, 742, 20
 Weisz, D. R. et al. 2011, *ApJ*, 739, 5
 Wolf, J., & Bullock, J. S. 2012, *ArXiv e-prints*
 Wolf, J., Martinez, G. D., Bullock, J. S., Kaplinghat, M., Geha, M., Muñoz, R. R., Simon, J. D., & Avedo, F. F. 2010, *MNRAS*, 406, 1220
 Zolotov, A. et al. 2012, *ArXiv e-prints*